Braz J Phys
DOI 10.1007/s13538-016-0419-2

ATOMIC PHYSICS

Solvent Effects on Molecular Structure, Vibrational Frequencies, and NLO Properties of N-(2,3-Dichlorophenyl) -2-Nitrobenzene–Sulfonamide: a Density Functional Theory Study

Nadia Benhalima[1] · **Nourdine Boukabcha**[1] · **Ömer Tamer**[2] · **Abdelkader Chouaih**[1] · **Davut Avcı**[2] · **Yusuf Atalay**[2] · **Fodil Hamzaoui**[1]

Received: 25 January 2016 /

Abstract Density functional theory (DFT) calculations have been performed to obtain optimized geometries, vibrational wavenumbers, highest occupied molecular orbital (HOMO)–lowest unoccupied molecular orbital (LUMO) energies, nonlinear optical (NLO), and thermodynamic properties as well as molecular surfaces for N-(2,3-dichlorophenyl)-2-nitrobenzene–sulfonamide in different solvents. B3LYP level gives similar results for geometric parameters and vibration frequencies in gas phase, water, and ethanol solvents. The most stable structure, which is defined by the highest energy gap between HOMO and LUMO, is obtained in gas phase ($\Delta E = 10.7376$ eV). Obtained small energy gaps between HOMO and LUMO demonstrate the high-charge mobility in the titled compound. The magnitude of first static hyperpolarizability (β) parameter increases by the decreasing HOMO–LUMO energy gap. The intensive interactions between bonding and antibonding orbitals of titled compound are responsible for movement of π-electron cloud from donor to acceptor, i.e., intramolecular charge transfer (ICT), inducing the nonlinear optical properties. So, the β parameter for title compound is found to be in the range of 5.5255–3.7187×10^{-30} esu, indicating the considerable NLO character. All of these calculations have been performed in gas phase as well as water and ethanol solvents in order to demonstrate solvent effect on molecular structure, vibration frequencies, NLO properties, etc.

Keywords DFT · Nonlinear optics · Vibration spectrum · HOMO–LUMO · Molecular surfaces

1 Introduction

Sulfonamides are known as a significant class of compounds in medicinal and pharmaceutical chemistry with several biological applications [1–4]. Many chemotherapeutically important sulfa drugs, like sulphadiazine, sulphathiazole, sulphamerazine, and sulfonamides, possess SO_2NH moiety which is an important toxophoric function [5]. The chemistry of sulfonamides has been known as synthons in the preparation of various valuable biologically active compounds [6, 7] used as antibacterial [8], protease inhibitor [9], diuretic [10], antitumor [11], and hypoglycemic [12].

There has been growing interest in using organic materials for nonlinear optical (NLO) devices, functioning as second harmonic generators, frequency converters, electro optical modulators, etc. because of the large second-order electric susceptibilities of organic materials. Since the second-order electric susceptibility is related to first hyperpolarizability, the search for organic chromophores with large first hyperpolarizability is fully justified. The organic compound displaying high hyperpolarizability are those containing an electron donating group and an electron withdrawing group interacting through a system of conjugated double bonds. In the case of sulfonamides, the electron withdrawing group is the sulfonyl group [13, 14].

Until today, a number of nitrobenzene sulfonamide derivates have been synthesized and their structural,

✉ Yusuf Atalay
yatalay@sakarya.edu.tr

[1] LTPS Laboratory, Department of Chemical Engineering, Faculty of Science and Technology, Mostaganem University, 27000 Mostaganem, Algeria

[2] Department of Physics, Arts and Sciences Faculty, Sakarya University, 54187 Sakarya, Turkey

Published online: 27 April 2016

spectroscopic, biological, and pharmacological properties have been investigated. Chaithanya et al. synthesized a series of nitrobenzene sulfonamide deriveates, and reported the crystal structures [15, 16]. Then, some transition metal complexes of nitrobenzene sulfonamide deriveates have been synthesized, and their crystal structures and vibration frequencies were reported by using experimental and theoretical methods [17, 18]. Karabacak et al. reported FT-IR and Raman spectra as well as DFT level calculations for 2-, 3-, and 4-nitrobenzenesulfonamide [19]. Considering that above studies, a number of paper report the crystal structure, vibration spectra as well as biological and pharmacological properties of nitrobenzene sulfonamide derivates. But, a limited number of papers for the theoretical approaches have been reported concerning these compounds. Additionally, the nonlinear optical properties, natural bond orbital analysis, molecular surfaces, and atomic charges for this class of molecular systems are neglected until now. In the present paper, the optimized geometry, vibration frequencies, highest occupied molecular orbital (HOMO) and lowest unoccupied molecular orbital (LUMO) energies, natural bonding orbital (NBO) analysis, molecular surfaces, thermodynamic parameters as well as Mulliken, NBO, and electrostatic potential (ESP) atomic charges have been investigated by using B3LYP in gas phase, ethanol, and water solvents. In recent years, among the computational methods calculating the electronic structure of molecular systems, DFT methods has been favorite one due to its great accuracy in reproducing the experimental values of molecular geometry, vibrational frequencies, atomic charges, dipole moment, thermodynamical properties, etc. [20–22].

2 Computational Details

The molecular structure optimization of the title compound and corresponding vibrational harmonic frequencies were calculated using hybrid B3LYP functional [23, 24] which consist of the Lee–Yang–Parr correlation functional in conjunction with a hybrid exchange functional first proposed by Becke and 6-31G (*d*,*p*) basis set [25] as implemented in Gaussian 09 [26]. GaussView 5 program was used to visualize the obtained theoretical data [27]. At the optimized structure of the examined molecule, no imaginary frequency modes were obtained proving that a true minimum on the potential energy surface was found. The HOMO and LUMO energies were calculated by using the time-dependent DFT (TD-DFT) method [28–31] in different solvents and gas phase starting from the ground-state geometry. Also, it is calculated in ethanol solution using the Polarizable Continuum Model (PCM) [30, 32, 33]. The NBOs were calculated using B3LYP/6-31G(*d*,*p*) level in order to understand various second-order interactions between the filled orbitals of one subsystem and vacant orbitals of another subsystem, which is a measure of the intramolecular delocalization or hyperconjugation [34]. The first-order hyperpolarizability was calculated using B3LYP/6-31G (*d*,*p*) basis set. And also, the effect of temperature on the thermodynamic parameters of entropy, heat capacity at constant pressure and enthalpy change of the titled compound in the range 100–1,000 K were determined. The atomic charges and molecular electrostatic surfaces were also investigated by means of B3LYP/6-31G (*d*,*p*) level of DFT.

3 Result and Discussion

3.1 Optimized Geometry

The structural parameters of N-(2,3-dichlorophenyl)-2-nitrobenzene–sulfonamide were calculated by using DFT/B3LYP level with 6-31G(*d*,*p*) basis set. The optimized molecular structure of the title compound is shown in Fig. 1a. The calculated geometric parameters such as bond lengths and angles for the title compound are summarized in Table 1. The title compound was synthesized and its crystal structure was reported by Chaithanya et al. [35]. When the X-ray structure of N-(2,3-dichlorophenyl)-2-nitrobenzene–sulfonamide is compared with its optimized counterparts (see Table 1), slight conformational discrepancies are observed between them. These slight discrepancies are originated due to the fact that the experimental results are reported for solid phase and the theoretical calculations are obtained for gas phase. In the solid state, the existence of a crystal field along with the intermolecular interactions, which result in the differences in bond parameters between the calculated and experimental values.

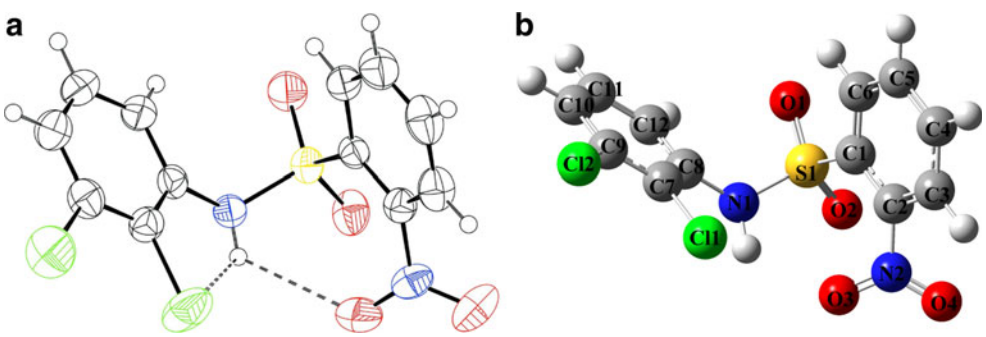

Fig. 1 **a** X-ray structure [30], **b** theoretical geometric structure in gas phase obtained at B3LYP/6-31G (*d*,*p*) level

The ring C–C bond lengths are calculated at the range of 1.390–1.411 Å in gas phase, and these bond lengths are reported at the region of 1.358 (4)–1.399 (3) Å. The C2–N2, C7–N1, and N1–S1 bond lengths are calculated at 1.475, 1.416, and 1.691 Å, respectively. The N2–O3 and N2–O4 bond lengths observed at 1.213 (3) and 1.220 (2) Å [35] are calculated at 1.231 and 1.225 Å. The geometric parameters obtained for gas phase are consistent with those calculated for water and ethanol solvents. In order to demonstrate the consistency among the results obtained for gas phase, ethanol, and water solvents, we calculated the root mean square deviation (R^2), and presented in Table 1. According to obtained R^2 values for bond lengths and angles, B3LYP level gives similar results for gas, ethanol, and water phases.

3.2 Nonlinear Optical Effects

Nonlinear optical (NLO) effects arise from the interactions of electromagnetic fields in various media to produce new fields altered in phase, frequency, amplitude, or other propagation characteristics from the incident fields [36]. NLO is at the forefront of current research because of its importance in providing the key functions of frequency shifting, optical modulation, optical switching, optical logic, and optical memory for the emerging technologies in areas such as telecommunications, signal processing, and optical interconnections [37–40]. In order to investigate the relationships among molecular structures and non-linear optical properties (NLO), the polarizabilities and first-order hyperpolarizabilities of the title compound were calculated using DFT/B3LYP method with 6-311G(*d*,*p*) basis set, based on the finite-field approach. The polarizability and hyperpolarizability tensors (α_{xx}, α_{xy}, α_{yy}, α_{xz}, α_{yz}, α_{zz} and β_{xxx}, β_{xxy}, β_{xyy}, β_{yyy}, β_{xxz}, β_{xyz}, β_{yyz}, β_{xzz}, β_{yzz}, β_{zzz}) can be obtained by a frequency job output file of Gaussian 09. The mean polarizability (α_{tot}) and the first-order hyperpolarizabiliy (β_{tot}) can be calculated using the following equations.

$$\alpha_{\text{tot}} = \frac{1}{3}\left(\alpha_{xx} + \alpha_{yy} + \alpha_{zz}\right) \tag{1}$$

$$\beta_{tot} = \left(\beta_x^2 + \beta_y^2 + \beta_z^2\right)^{\frac{1}{2}} \tag{2}$$

The complete equation for calculating the magnitude of first-order hyperpolarizability from Gaussian 09 output is given as follows:

$$\beta_{tot} = \left[\left(\beta_{xxx} + \beta_{xyy} + \beta_{xzz}\right)^2 + \left(\beta_{yyy} + \beta_{yzz} + \beta_{yxx}\right)^2 + \left(\beta_{zzz} + \beta_{zxx} + \beta_{zyy}\right)^2\right]^{\frac{1}{2}} \tag{3}$$

The calculated parameters described above and electronic dipole moment for title compound are listed in Table 2. The total dipole moment can be calculated using the following equation

$$\mu = \sqrt{\mu_x^2 + \mu_y^2 + \mu_z^2} \tag{4}$$

It is well-known that the higher values of dipole moment, molecular polarizability, and first-order hyperpolarizability are important for more active NLO properties. The mean polarizability (α_{tot}) and the first-order hyperpolarizability (β_{tot}) values for N-(2,3-dichlorophenyl)-2-nitrobenzene–sulfonamide are reported in Table 2. The polarizabilities and hyperpolarizability are reported in atomic units (a.u), the calculated values have been converted into electrostatic units (esu) (for α; 1 a.u = 0.1482×10^{-24}esu, for β; 1 a.u = 8.6393×10^{-33}esu). The calculated value of dipole moment is found to be 6.2747 Debye. The highest value of dipole moment is observed for component μ_x. In this direction, this value is equal to 6.1464 D. The calculated polarizability of the title compound is 2.7613×10^{-23} esu. The magnitude of the molecular hyperpolarizability β, is one of important key factors in a NLO system. The first hyperpolarizability value (β) of N-(2,3-dichlorophenyl)-2-nitrobenzene–sulfonamide calculated at B3LYP 6-31G(*d*,*p*) level is equal to 5.5255×10^{-30} esu. Considering that the first hyperpolarizability value for the p-Nitroaniline (pNA) [41, 42] commonly used as one of the prototypical molecule in the NLO studies was reported to be 14.39×10^{-30} esu, the title compound has considerable hyperpolarizability properties. As a consequently, the title compound can be good candidate to NLO material. In order to demonstrate solvent effect on NLO properties of title compound, μ, α, and β parameters have been examined in gas phase, water, and ethanol solvents. From Table 2, the magnitude of β parameter is ordered as water > ethanol > gas, as would be expected. The magnitude of μ shows a similar order, therefore it is demonstrated that the higher μ parameter implies the higher β.

3.3 HOMO–LUMO Analysis

HOMO and LUMO play a crucial role in the chemical stability of the molecule [43]. The HOMO as an electron donor represents the ability to donate an electron and LUMO as an electron acceptor represents the ability to accept an electron. The energy gap between HOMO and LUMO also determines the chemical reactivity, optical polarizability, and chemical

Table 1 Structural parameters calculated for N-(2,3-dichlorophenyl)-2-nitrobenzene–sulfonamide employing B3LYP method with6-31G (*d*,*p*) basis set

Bond distance (Å)	Experimental	Gas	Water ($\varepsilon = 78.39$)	Ethanol ($\varepsilon = 24.55$)
C1–C6	1.387 (3)	1.396	1.394	1.395
C1–C2	1.395 (3)	1.405	1.408	1.408
C1–S1	1.780 (2)	1.823	1.816	1.816
C2–C3	1.379 (3)	1.393	1.392	1.392
C2–N2	1.469 (3)	1.475	1.468	1.468
C3–C4	1.376 (3)	1.393	1.394	1.394
C4–C5	1.358 (4)	1.393	1.392	1.392
C5–C6	1.394 (3)	1.396	1.397	1.397
C7–C8	1.399 (3)	1.411	1.410	1.410
C7–N1	1.422 (3)	1.416	1.420	1.420
C7–C12	1.384 (3)	1.401	1.400	1.400
C8–C9	1.386 (3)	1.401	1.401	1.401
C8–Cl1	1.721 (2)	1.749	1.750	1.750
C9–C10	1.371 (3)	1.394	1.394	1.394
C9–Cl2	1.730 (2)	1.749	1.752	1.752
C10–C11	1.376 (4)	1.393	1.393	1.393
C11–C12	1.377 (3)	1.390	1.391	1.391
N1–S1	1.6287 (18)	1.691	1.692	1.692
N2–O3	1.213 (3)	1.231	1.234	1.234
N2–O4	1.220 (2)	1.225	1.227	1.227
O1–S1	1.4221 (16)	1.456	1.462	1.462
O2–S1	1.4236 (16)	1.462	1.464	1.464
R^2		0.992	0.991	0.992
Bond angle (°)				
C6–C1–C2	117.74 (19)	118.41	118.51	118.51
C6–C1–S1	116.24 (16)	115.77	115.75	115.75
C2–C1–S1	126.01 (15)	125.58	125.52	125.52
C3–C2–C1	121.70 (2)	120.99	120.92	120.93
C3–C2–N2	115.78 (19)	115.64	115.91	115.90
C1–C2–N2	122.49 (18)	123.34	123.14	123.15
C4–C3–C2	119.40 (2)	119.84	119.81	119.81
C5–C4–C3	120.10 (2)	119.81	119.86	119.86
C4–C5–C6	121.00 (2)	120.17	120.20	120.20
C1–C6–C5	120.00 (2)	120.76	120.67	120.67
C12–C7–C8	118.85 (19)	119.09	119.14	119.14
C12–C7–N1	120.83 (19)	120.18	119.93	119.94
C8–C7–N1	120.21 (18)	120.66	120.84	120.84
C9–C8–C7	119.83 (19)	119.84	119.69	119.69
C9–C8–Cl1	120.22 (17)	120.59	120.65	120.65
C7–C8–Cl1	119.92 (16)	119.57	119.65	119.65
C10–C9–Cl2	118.70 (18)	118.56	118.51	118.51
C8–C9–Cl2	120.55 (18)	120.97	120.85	120.85
C9–C10–C11	119.30 (2)	119.48	119.42	119.42
C12–C11–C10	121.00 (2)	120.74	120.62	120.63
C11–C12–C7	120.30 (2)	120.36	120.45	120.45
C7–N1–S1	122.60 (14)	123.31	122.66	122.68
O3–N2–O4	124.1 (2)	124.53	123.75	123.77
O3–N2–C2	118.64 (19)	118.24	118.55	118.54
O4–N2–C2	117.2 (2)	117.17	117.67	117.65
O1—S1–O2	119.54 (10)	121.65	120.13	120.19
O1–S1–N1	108.08 (10)	107.16	106.70	106.72
O2–S1–N1	106.41 (9)	107.00	107.03	107.02
O1–S1–C1	105.65 (10)	107.72	108.18	108.16
O2–S1–C1	110.21 (9)	105.64	106.36	106.33
N1–S1–C1	106.24 (9)	106.86	107.96	107.92
R^2		0.957	0.959	0.959

hardness–softness of the investigated systems [44, 45]. In the present study, the HOMO and LUMO energies are predicted at B3LYP method with 6-31G (*d*,*p*) basis set. According to the results, N-(2,3-dichlorophenyl)-2-nitrobenzene–sulfonamide contains 88 occupied molecular orbitals and 279 unoccupied virtual molecular orbitals. Figure 2 shows the distributions and energy levels of HOMO and LUMO orbitals for the title molecule in ethanol solvent. The frontier molecular gap values were found 10.7376, 3.8167, and 3.8180 eV for gas phase, water, and ethanol, respectively. This electronic absorption corresponds to the transition from the ground to the first excited state and is mainly described by one electron excitation from HOMO to LUMO. From Fig. 3, the HOMO is located over dichlorophenyl, NH, and SO_2 group. LUMO is located over the nitrobenzene. From Table 2, the HOMO–LUMO energy gap increases by the solvent order of water < ethanol < gas. Compared to occupied and unoccupied molecular orbitals in ethanol and water solvents, those for gas

Table 2 Total static dipol moment (μ, in Debye), the mean polarizability ($<\alpha>$, in 10^{-24} esu), the mean first-order hyperpolarizability ($<\beta>$, in 10^{-30} esu), and HOMO–LUMO energies (in electron volt) for N-(2,3–dichlorophenyl)-2-nitrobenzene–sulfonamide in gas phase, ethanol, and water solvents

Parameter	Gas	Water	Ethanol
μ	6.2747	8.3901	8.3020
$\alpha_{tot.}$	2.7613	3.7187	3.6821
$\beta_{tot.}$	5.5255	9.3713	9.1658
$E_{LUMO}+2$	2.8474	−0.9077	−0.9088
$E_{LUMO}+1$	2.3012	−1.4677	−1.4724
E_{LUMO}	1.2196	−3.0275	−3.0248
ΔE	10.7376	3.8167	3.8180
E_{HOMO}	−9.5180	−6.8442	−6.8428
$E_{HOMO}-1$	−9.6532	−7.0616	−7.0619
$E_{HOMO}-2$	−10.5895	−7.9043	−7.9103

phase found that the unoccupied molecular orbitals have higher energies while the occupied ones have lower energies. These results demonstrate that the electronic states for the titled compound show similarity in water and ethanol solvents. The magnitude of μ and β parameters increases by the decreasing HOMO–LUMO energy gap. That is, the small energy gap means that the titled compound has high charge mobility, inducing the dipole moment, and can be easily polarized (Fig. 3).

3.4 Molecular Electrostatic Potential

The molecular electrostatic potential (MEP) is related to the electronic density and is a very useful descriptor for determining the sites for electrophilic and nucleophilic reactions as well as hydrogen bonding interactions [46]. To predict reactive sites of electrophilic or nucleophilic attack for the investigated compound, MEP was calculated at the B3LYP/6-31G(*d*,*p*). The negative (red and yellow) regions of the MEP are related to electrophilic reactivity and the positive (blue) regions to nucleophilic reactivity, as shown in Fig. 2. As can be seen from Fig. 2, this molecule has several possible sites for electrophilic attack at O1, O2, O3, O4, Cl1, and Cl2 atoms of the title compound. The MEP shows that the negative potential sites are on electronegative atoms as well as the positive potential sites are around the hydrogen atoms. These sites give information about the region from where the compound can have intermolecular interactions.

3.5 Vibrational Assignments

We have calculated the theoretical vibrational spectra of N-(2,3-dichlorophenyl)-2-nitrobenzene–sulfonamide by using B3LYP method with 6-31G(*d*,*p*) basis set. None of the predicted vibrational spectra has any imaginary frequency, implying the optimized geometry is located at the local lowest point on the potential energy surface. DFT levels overestimate the vibrational wavenumbers due to the well-known systematic errors. So, the scaling factor of 0.9614 was used to calibrate calculated vibration frequencies [47]. The detailed

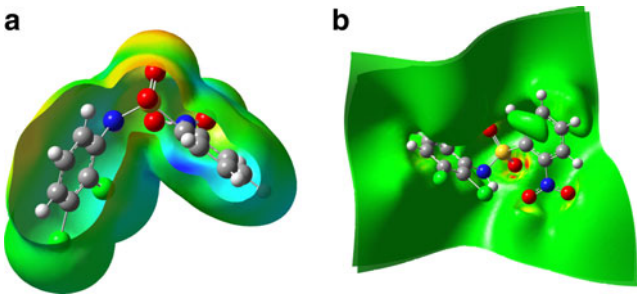

Fig. 2 **a** The electron density mapped with the molecular electrostatic potentials surface, **b** electrostatic potential (ESP) for N-(2,3-dichlorophenyl)-2-nitrobenzene–sulfonamide calculated in gas phase at B3LYP/6-31G (*d*,*p*) level

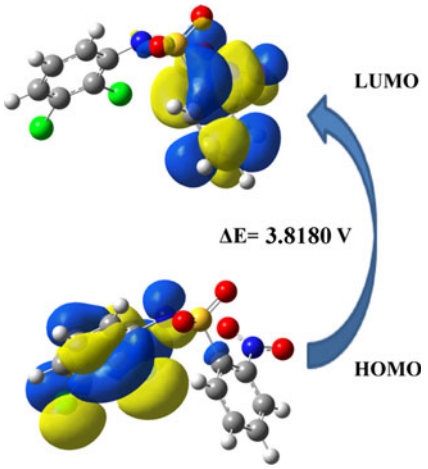

Fig. 3 HOMO and LUMO plot for N-(2,3-dichlorophenyl)-2-nitrobenzene–sulfonamide in ethanol solvent

assignments of vibration modes were provided by means of potential energy distribution (PED) analysis [48]. The detailed assignments and vibration frequencies for the title compound calculated in gas phase as well as water and ethanol solvents were presented in Table 3 as compared with each other. There are no significant discrepancies between the vibration frequencies obtained for gas phase, water, and ethanol solvents as readily seen Fig. 4. So, only gas phase vibration wavenumbers are discussed below.

3.5.1 N–H Vibrations

The N–H stretching vibrations occur in the region of 3,450–3,250 cm^{-1} [49]. In this study, the N–H stretching vibration wavenumber calculated by B3LYP/6-31G(*d*,*p*) method was found at 3,400 cm^{-1}. Based on the results of PED analysis shown in Table 3, N–H in plane bending (βHNC) vibrations at 1,428, 1,361, and 1,345 cm^{-1} with PED of 11–10 %. The N–H out of plane bending (ωHNCC) vibrations has been calculated at the range of 834–529 cm^{-1} with PED of 11–16 %.

3.5.2 C–H and C–C Vibrations

Aromatic structure shows the presence of C–H stretching vibration in the region 3,100–3,000 cm^{-1}. This is the characteristic region for the ready identification of C–H stretching vibrations [50]. In this region, the bands are not affected appreciably by the nature of the substituents. The C–H in plane bending (βCCH) vibrations appear in the range 1,300–1,000 cm^{-1} and out of plane bending (ωCCCH) vibrations occur in the range 1,000–750 cm^{-1} for substituted benzenes [51]. The vibration wavenumbers calculated at 1,598–1,014 cm^{-1} by using B3LYP/6-31G(*d*,*p*) method corresponds to C–H in plane bending vibrations with PED contribution range of 75-11 %. The C–H out of plane bending vibrations has been calculated at 976–394 cm^{-1} with the maximum PED

Table 3 Theoretical vibrational wavenumbers of N-(2,3-τichlorophenyl)-2-nitrobenzene–sulfonamite using B3LYP/6-31G(*d*,*p*) and their assignments

No.	ν (cm^{-1}) gas	ν (cm^{-1}) ethanol	ν (cm^{-1}) water	Assignments of normal modes with PED (%)
81	3,400	3,390	3,390	νNH(68)
80	3,128	3,126	3,126	νCH B (70)
79	3,117	3,123	3,123	νCH A (80)
78	3,112	3,119	3,120	νCH A(77)
77		3,108	3,108	νCH B (81)
76	3,094	3,105	3,105	νCH A(82)
75	3,082	3,093	3,093	νCH B (78)
74	3,080	3,091	3,091	νCH A(79)
73	1,598	1,582	1,582	ν_{as}NO2 (15), νCC A(17), βCCH A(19)
72	1,570	1,567	1,567	νCC B(31), βCCH B(29), βCCC B(14)
71	1,569	1,562	1,562	νCC A(23), βCCH A(32), βCCC A(10)
70	1,561	1,554	1,554	νCC A(24), βCCH A(24), βCCC A(10)
69	1,556	1,546	1,545	νCC B(24), βCCH B(23), βCCC B(11)
68	1,442	1,441	1,441	νCC A(20), βCCH A(50)
67	1,433	1,430	1,430	νCC B(15), βCCH B(35)
66	1,428	1,425	1,424	νCC B(12), βCCH B(19), βCCH A(10), βHNC (10)
65	1,419	1,418	1,418	νCC A(11), βCCH A(37)
64	1,361	1,353	1,352	νCC B(10), βCCH B(13),βHNC (11)
63	1,345	1,337	1,336	$\nu_s NO_2$ (11), βHNC (10)
62	1,309	1,311	1,311	νCC A(34), βCCH A(22)
61	1,290	1,271	1,270	νCC A(10), νCC B(18), ν_{as}SO2 (13)
60	1,256	1,251	1,250	νCC B(31), βCCH B(13)
59	1,245	1,241	1,241	νCN1(10), βCCH B(26), βCCH A(13)
58	1,238	1,237	1,237	βCCH A(39)
57	1,170	1,166	1,166	βCCH B(44), νCC B(14)
56	1,149	1,148	1,148	νCC A(12), βCCH A(75)
55	1,138	1,133	1,133	νCC B(19), βCCH B(41), νCCl2 (10)
54	1,126	1,126	1,126	νCN2(10), νCC A(17), βCCH A(42)
53	1,108	1,103	1,103	νCS (11), νCC A(14), $\nu_s SO_2$ (10), βCCH A(21)
52	1,086	1,081	1,081	νCC A(10), βCCH A(18)
51	1,084	1,079	1,078	νCC B(14), βCCH B(28)
50	1,029	1,029	1,029	νCC A(20), βCCH A(30), βCCC A(13)
49	1,017	1,013	1,013	νCCl1 (10), νCC B(13), βCCH B(11), βCCC B(24)
48	1,014	1,011	1,010	βCCH A(15), βCCC A(24)
47	976	986	986	ωCCCH A(71),ωCCCC A(12)
46	949	953	953	ωCCCH A(57)
45	945	951	952	ωCCCH B(70), ωCCCC B(11)
44	896	889	889	ωCCCH B(23), βCCC B(10)
43	878	879	879	ωCCCH B(48)
42	874	874	874	ωCCCH A(55)
41	834	832	832	βCCC A(14), βNO2 (18), ωHNCC (11)
40	810	814	814	ωCCCH B(18)
39	774	773	773	ωCCCH A(48)
38	759	758	758	ωCCCH B(40), βCCC B(11)
37	726	723	723	ωCCCH A(30), βCCC A(16)
36	718	714	714	βCCC B(17)
35	710	707	707	ωCCCH A(23), βCCC A(16)
34	687	686	686	ωCCCH B(14), βCCC B(25)
33	674	671	671	ωCCCH A(17), ωCCCC A(21), βCCC B(11)

Table 3 (continued)

No.	ν (cm^{-1}) gas	ν (cm^{-1}) ethanol	ν (cm^{-1}) water	Assignments of normal modes with PED (%)
32	657	650	650	ωCCCH B(10), βCCC B(13), ωHNCC (11)
31	635	632	632	βCCC A(21)
30	589	574	574	τSONH(14), ωHNCC (16)
29	555	553	553	ωCCCH A(13), ωCCCC A(12)
28	548	546	546	ωCCCH B(12)
27	529	518	518	τSONH(11), ωHNCC (13)
26	517	511	510	ωCCCH B(10)
25	497	496	496	ωCCCH B(20), ωCCCC B(26)
24	481	479	479	ωCCCH A(12), ωCCCC A(11)
23	454	451	451	ωCCCC A(10)
22	440	439	439	ωCCCH A(10), ωCCCC A(11)
21	411	411	411	ωCCCH A(23), ωCCCC A(19)
20	394	395	395	ωCCCH A(18), ωCCCC A(18)
19	375	375	375	βCH B(12)
18	344	344	344	ωCCC B(11)
17	306	305	305	ωCCC A(10)
16	284	285	285	ωCCC B(10)
15	259	260	260	τSOCC (12)
14	245	244	244	τClCCC(16)
13	237	239	239	τClCCC(15)
12	218	216	216	τClCCC(17), ωCCCC B(12)
11	205	206	206	τClCCC(15)
10	205	205	204	τClCCC(12)
9	172	175	175	τCCNO2(13)
8	147	145	145	τCCCN1(10), τSOCC (10)
7	130	128	128	τSOCC (11), τClCCC(12)
6	101	101	101	τCCNO2(16), τSOCC (10)
5	86	81	81	τCCNO2(28)
4	63	63	63	τCCNO2(15), τClCCC(11)
3	38	38	38	τSOCC (20), τCCNO2(32)
2	21	23	23	τCSNC(10),τCNSO(19),τCCNS(11)
1	16	16	16	τSONH(11), τCCNS(21)

ν stretching, β in-plane bending, ω out-of-plane bending, τ deformation, *s* symmetric, *as* asymmetric

contribution of 71 %. The ring stretching vibrations are very much important in the spectrum of aromatic compounds and are highly characteristic of the aromatic ring itself. However, empirical assignments of vibrational modes for peaks in the fingerprint region are difficult. Bands between 1,400 and 1, 650 cm^{-1} in benzene derivatives are assigned to ring vibrations [52, 53]. The bands at the range of 1,598–1,017 cm^{-1} have been assigned as the C–C stretching vibrations.

3.5.3 NO_2 Vibrations

For the molecules having nitro group, the NO_2 asymmetric stretching band is expected in the region 1,625–1,540 cm^{-1} and that of symmetric stretching vibration is expected in the region 1,400–1,360 cm^{-1} [54]. The asymmetric stretching mode of NO_2 bond are calculated at 1,598 cm^{-1} with PED of 15 % .The NO_2 symmetric stretching mode is calculated at 1,345 cm^{-1} by with PED of 11 % by using B3LYP method. The nitro group is capable of different bending vibration such as scissoring, wagging, rocking, and twisting and these vibrations give rise to several variable intensity bands at lower wavenumber. The NO_2, in-plane deformation vibrations are expected in region 775–662 cm^{-1} [55]. The vibration wavenumber calculated at 834 cm^{-1} was designated as NO_2 in plane bending vibrations with PED of 18 %.

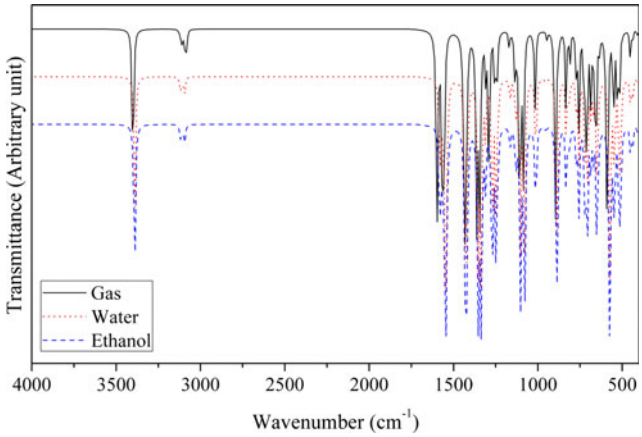

Fig. 4 Simulated infrared spectra of N-(2,3-dichlorophenyl)-2-nitrobenzene–sulfonamide in gas phase, water, and ethanol solvents

3.5.4 SO_2 Vibrations

The asymmetric stretching vibrations for the SO_2, NH_2, NO_2, CH_2, and CH_3, etc. has magnitude higher than the symmetric stretching [56, 57]. The symmetric and asymmetric SO_2 stretching vibrations occur in the region 1,125–1,150 and 1,295–1,330 cm^{-1}, respectively [58]. In the present study, the symmetric S = O stretching vibrations is assigned at 1,108 cm^{-1} with the PED contribution of 10 %. The S = O asymmetric stretching mode is predicted by B3LYP/6-31G (*d*,*p*) method at 1,290 cm^{-1} with the PED contribution of 13 %.

3.5.5 C–N, C–Cl, and C–S Vibrations

Because of the mixing of several bands, the identification of C–N vibrations in IR spectrum is a very difficult task.

Table 4 Atomic charges (*e*) of the title compound in gas phase and solution phase obtained at B3LYP/6-31G(*d*,*p*)

Atoms	Gas phase			Ethanol			Water		
	Mulliken	NBO	ESP	Mulliken	NBO	ESP	Mulliken	NBO	ESP
C1	−0.195689	−0.31229	−0.080117	−0.191854	−0.31744	−0.023520	−0.191795	−0.31716	−0.025333
C2	0.251079	0.07729	−0.023893	0.259664	0.07413	−0.044817	0.259917	0.07429	−0.043269
C3	0.082455	−0.20824	−0.104112	−0.060912	−0.19872	−0.065578	−0.060718	−0.19911	−0.068441
C4	0.030209	−0.21323	−0.053696	−0.090403	−0.20359	−0.056675	−0.090246	−0.20404	−0.051777
C5	0.059942	−0.20455	−0.112011	−0.058672	−0.19311	−0.055788	−0.058497	−0.19363	−0.057599
C6	0.052861	−0.21195	−0.033520	−0.099631	−0.20618	−0.045249	−0.099443	−0.20643	−0.044408
C7	−0.125609	−0.08429	−0.076596	−0.115900	−0.08046	−0.081623	−0.115629	−0.08056	−0.082199
C8	0.256810	0.1257	0.421503	0.255850	0.12307	0.377720	0.255827	0.12319	0.378814
C9	−0.104011	−0.06035	0.140495	−0.106412	−0.06091	−0.081623	−0.106464	−0.06092	0.126966
C10	0.058558	−0.24633	−0.165397	−0.061972	−0.24192	−0.158565	−0.061965	−0.24212	−0.155565
C11	0.008946	−0.22135	−0.052918	−0.105406	−0.21901	−0.025451	−0.105475	−0.21916	−0.025482
C12	0.086389	−0.22828	−0.289546	−0.054868	−0.22772	−0.253547	−0.055080	−0.22767	−0.252940
N1	−0.367745	−0.88932	−0.724033	−0.705811	−0.89167	−0.613624	−0.705942	−0.89159	−0.616414
N2	0.382919	0.52535	0.823193	0.381820	0.52989	0.701635	0.381672	0.52978	0.702111
O1	−0.539452	−0.94562	−0.549879	−0.552199	−0.95675	−0.455831	−0.552578	−0.95641	−0.457215
O2	−0.502302	−0.91032	−0.551407	−0.541312	−0.94442	−0.474255	−0.542808	−0.94317	−0.477145
O3	−0.394824	−0.38835	−0.464037	−0.413818	−0.40661	−0.407873	−0.414552	−0.40589	−0.408701
O4	−0.539452	−0.35235	−0.444522	−0.383832	−0.36965	−0.399378	−0.384530	−0.36908	−0.400633
Cl1	0.028562	0.03046	−0.099594	0.022691	0.02634	−0.083680	0.022527	0.02646	−0.083287
Cl2	0.017704	0.02751	−0.117015	0.002720	0.01577	−0.119062	0.002260	0.01612	−0.119652
S	1.276253	2.35893	1.133899	1.265239	2.35713	0.833899	1.264682	2.35725	0.837989
H1	0.335753	0.46091	0.420487	0.338879	0.46135	0.382304	0.338910	0.46139	0.382696
H3	0.147104	0.27888	0.151003	0.159879	0.28584	0.140283	0.160316	0.28561	0.141485
H4	0.120317	0.25803	0.120427	0.146029	0.27266	0.125057	0.146966	0.27213	0.124373
H5	0.118938	0.25764	0.133061	0.144449	0.27204	0.127545	0.145381	0.27152	0.128645
H6	0.156564	0.28395	0.116827	0.161100	0.28627	0.112270	0.161275	0.28619	0.112243
H10	0.118084	0.26264	0.138859	0.137865	0.27306	0.137179	0.138544	0.27271	0.136420
H11	0.109259	0.25417	0.129198	0.131433	0.26630	0.117754	0.132177	0.26590	0.136420
H12	0.136609	0.27536	0.213343	0.135383	0.27434	0.181179	0.135267	0.27441	0.117689

Shanmugam [59] assigned C–N stretching absorption in the region 1,382–1,266 cm^{-1}. In the present work, the calculated wavenumbers at 1,245 and 1,126 cm^{-1} (mode nos. 59 and 54) are assigned to C–N stretching vibrations. The vibration belonging to the bond between the ring and halogen atoms will be discussed here. Balachandran et al. [60] assigned vibrations of C–X group (X = F, Cl, and Br) in the frequency range 1, 292–485 cm^{-1}. The wavenumber of C–Cl stretching vibrations are calculated at 1,184 and 1,058 cm^{-1} by B3LYP/6-31G(*d*,*p*) level. It is difficult to designate the C–S stretching vibration in different compounds, since this vibration has variable intensity and may be found over the wide region 1,035–245 cm^{-1} both in aliphatic and aromatic molecules [61–63]. The theoretically scaled wavenumber obtained at 1,152 cm^{-1} corresponds to C–N stretching vibrations with PED of 10 %.

3.6 Mulliken NBO and ESP Population Analysis

Mulliken, natural bond orbital (NBO), and electrostatic potential (ESP) atomic charges of the title compound were calculated by using B3LYP/6-31G(*d*,*p*) level in gas-phase, ethanol, and water solvents and presented in Table 4. The ESP atomic charges in gas phase, ethanol, and water solvents are also presented in Fig. 5, as compared with each other. ESP atomic charges presented in Fig. 5 show that the O1, O2, and N1 atoms of sulfonamide group, O3 and O4 atoms of nitro group have larger negative atomic charges than the rest of atoms in gas phase, ethanol, and water solvents. On the other hand, it is found that in Table 4 and Fig. 5, the atomic charge values of the N1, O1, O2, and O3 atoms in solution phase are larger than those in gas phase, and while their atomic charge values increase with the increase of the polarity of the solvent, that value of O4 decrease with the increasing polarity of the solvent. The charge on H1 atom has the maximum magnitude of 0.420487, 0.382304, and 0.382696 in gas phase, ethanol, and water solvents. The obtained atomic charges for H1 are larger than the other H atoms due to the hydrogen bonding interaction. This clearly indicates the presence of intra molecular hydrogen bonding (N–H···Ol).However, all the hydrogen atoms exhibit net positive charges and these magnitudes are changing between 0.109259 and 0.46139. From Fig. 5, the higher positive charges are found at S, N2, and C8 atoms for N-(2,3-dichlorophenyl)-2-nitrobenzene–sulfonamide molecule.

3.7 Thermodynamic Properties

The correlations between the statistical thermodynamics and temperature were obtained by using B3LYP level. It is seen that the heat capacities, entropies, and enthalpies increase with the increasing temperature since the intensity of the molecular vibrations increase with temperature. The standard heat capacities, standard entropies, and standard enthalpy changes were obtained and are listed in Table 5. As can be seen from Table 5, the standard heat capacities, entropies, and enthalpy changes at any temperature from 100 to 1,000 K because increasing the temperature causes an increase in the intensity of the molecular vibration. The correlation graphs are shown in Fig. 6. All the thermodynamic data supply helpful information for the further study on the N-(2,3-dichlorophenyl)-2-nitrobenzene–sulfonamide. They can be used to compute the other thermodynamic energies according to relationships of thermodynamic functions and estimate directions of chemical reactions according to the second law of thermodynamics in thermochemical field [64].

3.8 NBO Analysis

Natural bond orbital (NBO) analysis is an essential tool for studying intra- and intermolecular bonding and interaction among bonds, and also provides a convenient basis for investigating charge transfer or conjugative interaction in molecular

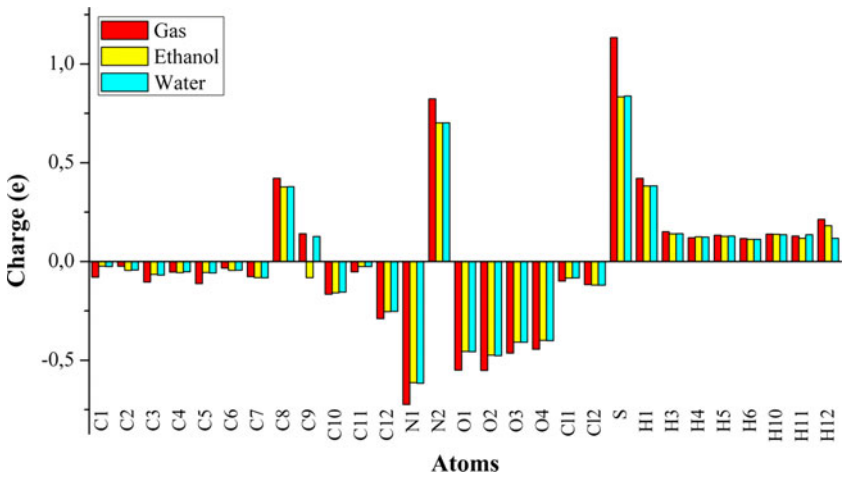

Fig. 5 The electrostatic potential (ESP) atomic charges for the title compound

Table 5 Thermodynamic properties at different temperatures at the B3LYP/6-31G(*d*,*p*) level for N-(2,3-dichlorophenyl)-2-nitrobenzene–sulfonamide in gas phase

T (K)	*S* (J/mol·K)	Cp (J/mol·K)	Δ*H* (kJ/mol)
100	332.19	98.29	5.97
200	426.41	183.1	20.05
293.15	510.06	258.05	40.65
298.15	514.45	261.84	41.95
300	516.08	263.24	42.43
400	601.58	332.24	72.32
500	681.91	387.59	108.42
600	756.56	430.8	149.43
700	825.61	464.66	194.27
800	889.48	491.63	242.14
900	948.7	513.5	292.43
1,000	1,003.76	531.51	344.71

systems. NBO analysis is performed for the title compound using B3LYP method and 6-31G(*d*,*p*) basis set in order to elucidate the intramolecular interactions, hybridization, and delocalization of electron density. The second-order Fock matrix was carried out to evaluate donor (*i*)–acceptor (*j*), i.e., donor level bonds to acceptor level bonds interaction in the NBO analysis [65–68]. The result of interaction is a loss of occupancy from the concentration of electron NBO of the idealized Lewis structure into an empty non-Lewis orbital. For each donor (*i*) and acceptor (*j*), the stabilization energy $E^{(2)}$ associates with the delocalization $i \rightarrow j$ is estimated as

$$E^{(2)} = \Delta E_{ij} = q_i \frac{F(i,j)^2}{\varepsilon_j - \varepsilon_i} \quad (5)$$

where q_i is the donor orbital occupancy, are ε_j and ε_i diagonal elements and $F(i,j)$ is the off diagonal NBO Fock matrix element. The larger $E^{(2)}$ value the more intensive is the interaction between electron donors and acceptor, i.e., the more donation tendency from electron donors to electron acceptors and the greater the extent of conjugation of the whole system. The strong intramolecular hyperconjugative interaction of the σ and π electrons of C–C to the anti C–C bond of the benzene ring leads to stabilization of some part of the benzene ring as evident from Table 6. For example, the intramolecular hyperconjugative interaction of σ(C1–C6) distributes to σ(C1–C2) and σ(C2–N1) leading to stabilization of 4.39 and 5.12 kcal/mol, respectively. This enhances further conjugation with antibonding orbitals of π(C2–C3) and π(C4–C5) which leads to strong delocalization of 20.24 and 17.27 kcal/mol, respectively. This interaction around the ring can induce larger bioactivity in the molecule. The intramolecular interaction π(C2–C3) → π(C4–C5), π(C2–C3) → π(N2–O4), π(C4–C5) → π(C1–C6), and π(C7–12) → π(C10–C11) energies have been found to be 17.26, 20.75, 22.78, and 20.25 kcal/mol, respectively. These large intramolecular interaction energies are indicator of the intramolecular charge transfer (ICT). The most important interaction energy in the title compound is from electron donating LP(3) O3 to the anti-bonding (N2–O4) resulting stabilization of 154.04 kcal/mol. The movement of π-electron cloud from donor to acceptor, i.e., intramolecular charge transfer (ICT) can make the molecule more polarized and the ICT must be responsible for the NLO properties of molecule. Therefore, the titled compound may be used for non-linear optical materials application in future.

4 Conclusion

The optimized geometry and vibrational wavenumbers for N-(2,3-dichlorophenyl)-2-nitrobenzene–sulfonamide has been obtained by using B3LYP/6-31G(*d*,*p*) level. It was noted here that the experimental results belong to solid phase and theoretical calculations belong to gas phase. Despite the different phases, geometric parameters obtained at B3LYP method are in a good agreement with experimental ones. The molecular electrostatic potential (MEP) map shows that the negative potential sites are on the electronegative atoms as well as the positive potential sites are around the hydrogen atoms.

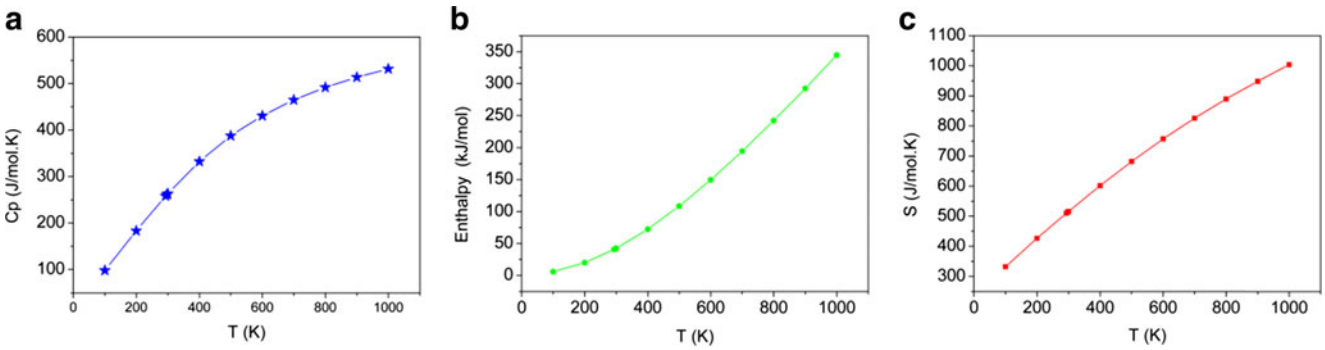

Fig. 6 **a** Temperature dependence of heat capacity at constant pressure (*Cp*), **b** temperature dependence of enthalpy (H), **c** Temperature dependence of entropy (*S*) of the title compound in gas phase

Table 6 Second order perturbation theory analysis of Fock matrix in NBO basis for N-(2,3-dichlorophenyl)-2-nitrobenzene–sulfonamide

Donor (*i*)	Type	ED (e)	Acceptor (*j*)	Type	ED (e)	$E^{(2)}$ (kcal/mol)	$E(j)$–$E(i)$ (a.u.)	$F(i, j)$ (a.u.)
C1–C2	σ	1.97531	C2–C3	σ^*	0.02145	4.10	1.3	0.065
C1–C6	σ	1.97259	C1–C2	σ^*	0.03149	4.39	1.26	0.066
C1–C6	σ		C2–N2	σ^*	0.10460	5.12	1.00	0.065
C1–C6	π		C2–C3	π^*	0.34979	20.24	0.29	0.068
C1–C6	π	1.67603	C4–C5	π^*	0.29514	17.27	0.3	0.064
C1–C6	π		N1–S1	σ^*	0.26319	4.49	0.41	0.039
C2–C3	σ	1.97028	C1–C2	σ^*	0.03149	5.09	1.26	0.071
C2–C3	π		C4–C5	π^*	0.29514	17.26	0.3	0.065
C2–C3	π		N2–O4	π^*	0.59963	20.75	0.16	0.055
C4–C5	π	1.62999	C1–C6	π^*	0.34319	22.78	0.27	0.07
C4–C5	π		C2–C3	π^*	0.34979	22.81	0.27	0.071
C7–C8	σ	1.97149	C8–C9	σ^*	0.04080	4.28	1.26	0.066
C7–C8	σ		C9–Cl2	σ^*	0.02621	4.07	0.88	0.053
C7–C12	σ	1.96939	C7–C8	σ^*	0.03964	4.05	1.23	0.063
C7–C12	σ		C8–Cl1	σ^*	0.02540	4.24	0.84	0.054
C7–C12	π	1.64078	C8–C9	π^*	0.46767	21.23	0.25	0.067
C7–C12	π		C10–C11	π^*	0.33542	20.25	0.29	0.069
C7–C12	π		N1–S29	σ^*	0.26319	4.15	0.39	0.037
C8–C9	π	1.71238	C7–C12	π^*	0.37648	17.24	0.31	0.067
C8–C9	π		C10–C11	π^*	0.33542	16.25	0.32	0.065
C9–C10	σ	1.97520	C8–C9	σ^*	0.04080	4.52	1.26	0.067
C9–C10	σ		C8–Cl1	σ^*	0.02540	4.40	0.86	0.055
N2–O4	π		N2–O4	π^*	0.59963	6.76	0.33	0.05
N1	LP(1)	1.82997	C1–S1	σ^*	1.44721	8.97	0.44	0.057
N1	LP(1)		C7–C8	σ^*	0.03964	4.54	0.83	0.057
N1	LP(1)		C7–C12	π^*	0.37648	12.88	0.33	0.061
O1	LP(2)	1.80751	C1–S1	σ^*	1.44721	18.99	0.42	0.081
O1	LP(2)		N1–S1	σ^*	0.26319	11.53	0.42	0.063
O1	LP(3)	1.78863	N1–S1	σ^*	0.26319	13.98	0.42	0.069
O1	LP(3)		O2–S1	σ^*	0.14837	19.83	0.58	0.097
O2	LP(2)	1.80052	C1–S1	σ^*	1.44721	21.50	0.41	0.085
O2	LP(3)	1.76683	N1–S1	σ^*	0.26319	18.74	0.41	0.079
O2	LP(3)		O1–S1	σ^*	0.15006	18.48	0.56	0.093
O3	LP(2)	1.89521	C2–N2	σ^*	0.10460	10.77	0.57	0.07
O3	LP(2)		N2–O4	σ^*	0.05821	19.89	0.72	0.108
O3	LP(3)		N2–O4	π^*	0.59963	154.04	0.15	0.14
O4	LP(2)	1.89125	C2–N2	σ^*	0.10460	13.50	0.56	0.078
O4	LP(2)		N2–O3	σ^*	0.06657	19.64	0.70	0.106
Cl1	LP(3)	1.96054	C8–C9	π^*	0.46767	13.07	0.31	0.064
Cl2	LP(3)	1.92556	C8–C9	π^*	0.46767	14.02	0.30	0.065

$E^{(2)}$ is the energy of hyperconjugative interactions

$E(j) - E(i)$ Energy difference between donor and acceptor i and j NBO orbitals

$F(i, j)$ is the Fock matrix element between i and j NBO orbitals

These sites give information about the possibleareas for inter- and intramolecular hydrogen bonding. The lowering of HOMO–LUMO energy gap clearly explains the charge transfer interactions taking place within the molecule. HOMO–LUMO energy gap is reduced by the solvent order of water < ethanol < gas. The reducing energy gap means that the title compound can be easily polarized, and have higher first-order hyperpolarizability. Stability of the molecule

arising from hyper conjugative interactions and charge delocalization have been analyzed using natural bond orbital (NBO) analysis. The high stabilization energies demonstrate that the charge transfer occurs in the title compound.

References

1. S.A. Tilles, South Med J **94**, 817 (2001)
2. C.G. Slatore, S. Tilles, Immunol Allergy Clin N Am **24**, 477 (2004)
3. C.C. Brackett, H. Singh, J.H. Block, Pharmacotherapy **24**, 856 (2004)
4. E. Eroglu, Int J Mol Sci **9**, 181 (2008)
5. A.M. Badawi, H. El-Sharkawy Ali, D.A. Ismail, Aust J Basic Appl Sci **2**, 301 (2008)
6. Z. Guo, P.J. Sadler, Angew Chem Int Ed Engl **38**, 1512 (1999)
7. R.X. Yuan, R.G. Xiong, Z.F. Chen, P. Zhang, H.X. Ju, Z. Dai, Z.J. Guo, H.K. Fun, X.Z. You, J Chem Soc Dalton Trans **6**, 774 (2001)
8. T.H. Maren, Annu Rev Pharmacol Toxicol **16**, 309 (1976)
9. C.T. Supuran, A. Scozzafava, A. Mastrolorenzo, Exp Opin Ther Pat **111**, 221 (2000)
10. A.E. Boyd, Diabetes **37**, 847 (1988)
11. T. Owa, T. Nagasu, Exp Opin Ther Pat **10**, 1725 (2000)
12. A. Chandran, H.T. Varghese, Y.S. Mary, C.Y. Panicker, T.K. Manojkumar, C. Van Alsenoy, G. Rajendran, Spectrochim Acta Part A **87**, 29 (2012)
13. X. Liu, L. Liu, X. Lu, J. Zheng, W. Wang, Y. Fang, Thin Solid Films **217**, 174 (1992)
14. Y. Miyamoto, K. Kaifu, T. Koyano, M. Saito, M. Kato, Thin Solid Films **210–211**, 178 (1992)
15. U. Chaithanya, S. Foro, B.T. Gowda, Acta Cryst E **68**, 2576 (2012)
16. U. Chaithanya, S. Foro, B.T. Gowda, Acta Cryst E **68**, 2577 (2012)
17. G. Camí, E. Chacón Villalba, Y. Di Santi, P. Colinas, G. Estiu, D.B. Soria, J Mol Struct **995**, 72 (2011)
18. G. Estiu, M.E. Chacón Villalba, G.E. Camí, G.A. Echeverria, D.B. Soria, J Mol Struct **1062**, 82 (2014)
19. M. Karabacak, E. Postalcılar, M. Çınar, Spectrochim Acta A **85**, 261 (2012)
20. G.S. Kürkçüoğlu, E. Sayın, K. Gör, T. Arslan, O. Büyükgüngör, Vib Spectrosc **71**, 105 (2014)
21. E. Temel, C. Alaşalvar, H. Gökçe, A. Güder, Ç. Albayrak, Y. Bingöl Alpaslan, G. Alpaslan, N. Dilek, Spectrochim Acta A **136**, 534 (2015)
22. Ü. Ceylan, G. Özdemir Tarı, H. Gokçe, E. Ağar, J Mol Struct **1110**, 1 (2016)
23. C. Lee, W. Yang, R.G. Parr, Phys Rev B **37**, 785 (1988)
24. A.D. Becke, J Chem Phys **98**, 5648 (1993)
25. M.J. Frisch, J.A. Pople, R. Krishnam, J.S. Binkley, J Chem Phys **80**, 3265 (1984)
26. M.J. Frisch, G.W. Trucks, H.B. Schlegel, G.E. Scuseria, M.A. Robb, J.R. Cheeseman, G. Scalmani, V. Barone, B. Mennucci, G.A. Petersson, H. Nakatsuji, M. Caricato, X. Li, H.P. Hratchian, A.F. Izmaylov, J. Bloino, G. Zheng, J.L. Sonnenberg, M. Hada, M. Ehara, K. Toyota, R. Fukuda, J. Hasegawa, M. Ishida, T. Nakajima, Y. Honda, O. Kitao, H. Nakai, T. Vreven, J.A. Montgomery Jr., J.E. Peralta, F. Ogliaro, M. Bearpark, J.J. Heyd, E. Brothers, K.N. Kudin, V.N. Staroverov, R. Kobayashi, J. Normand, K. Raghavachari, A. Rendell, J.C. Burant, S.S. Iyengar, J. Tomasi, M. Cossi, N. Rega, J.M. Millam, M. Klene, J.E. Knox, J.B. Cross, V. Bakken, C. Adamo, J. Jaramillo, R. Gomperts, R.E. Stratmann, O. Yazyev, A.J. Austin, R. Cammi, C. Pomelli, J.W. Ochterski, R.L. Martin, K. Morokuma, V.G. Zakrzewski, G.A. Voth, P. Salvador, J.J. Dannenberg, S. Dapprich, A.D. Daniels, O. Farkas, J.B. Foresman, J.V. Ortiz, J. Cioslowski, D.J. Fox, *Gaussian 09, revision A.1* (Gaussian, Inc, Wallingford, 2009)
27. R. Dennington, T. Keith, J. Millam, *Gauss view, version 5* (Semichem Inc, Shawnee Mission, 2009)
28. S. Miertuš, E. Scrocco, J. Tomasi, Chem Phys **55**, 117 (1981)
29. S. Miertuš, J. Tomasi, Chem Phys **65**, 239 (1982)
30. J. Tomasi, B. Mennucci, R. Cammi, Chem Rev **105**, 2999 (2005)
31. R. Ditchfield, Chem Phys **76**, 5688 (1972)
32. B. Mennucci, J. Tomasi, J Chem Phys **106**, 5151 (1997)
33. M. Cossi, V. Barone, M.A. Robb, J Chem Phys **111**, 5295 (1999)
34. E.D. Glendening, A.E. Reed, J.E. Carpenter, F. Weinhold, *NBO version 3.1, TCI* (University of Wisconsin, Madison, 1998)
35. U. Chaithanya, F. Sabine, B. Thimme Gowda, Acta Cryst **E69**, o76 (2013)
36. Y.X. Sun, Q.L. Hao, W.X. Wei, Z.X. Yu, L.D. Lu, X. Wang, Y.S. Wang, J Mol Struct:Theochem **904**, 74 (2009)
37. C. Andraud, T. Brotin, C. Garcia, F. Pelle, P. Goldner, B. Bigot, A. Collet, J Am Chem Soc **116**, 2094 (1994)
38. V.M. Geskin, C. Lambert, J.L. Bredas, J Am Chem Soc **125**, 15651 (2003)
39. N. Dege, N. Şenyüz, H. Batı, N. Günay, D. Avcı, Ö. Tamer, Y. Atalay, Spectrochim Acta A **120**, 323 (2014)
40. N. Öner, Ö. Tamer, D. Avcı, Y. Atalay, Spectrochim Acta A **133**, 542 (2014)
41. L.T. Cheng, W. Tam, S.H. Stevenson, G.R. Meredith, G. Rikken, S.R. Marder, J Phys Chem **95**, 10631 (1991)
42. P. Kaatz, E.A. Donley, D.P. Shelton, J Chem Phys **108**, 849 (1998)
43. S. Gunasekaran, R.A. Balaji, S. Kumeresan, G. Anand, S. Srinivasan, Can J Anal Sci Spectrosc **53**, 149 (2008)
44. H. Pir Gümüş, Ö. Tamer, D. Avcı, Y. Atalay, Spectrochim Acta A **129**, 219 (2014)
45. H. Pir Gümüş, Ö. Tamer, D. Avcı, Y. Atalay, Spectrochim Acta A **132**, 183 (2014)
46. N. Okulik, A.H. Jubert, Int Electron J Mol Des **4**, 17 (2005)
47. J.B. Foresman, Exploring chemistry with electronic structure methods, in *A guide to using gaussian*, ed. by E. Frisch (Gaussian Inc, Pittsburg, 1996)
48. A. Pekparlak, D. Avcı, Y. Atalay, K. Esmer, Arab J Sci Eng **37**, 171 (2012)
49. M. Silverstein, G.C. Bassler, C. Morril, *Spectroscopic identification of organic compounds* (John Wiley, New York, 1981)
50. J. Mohan, *Organic spectroscopy principles and applications*, 2nd edn. (Narosa Publishing House, New Delhi, 2001)
51. G. Socrates, *Infrared and raman characteristics group frequencies*, 3rd edn. (Wiley, New York, 2001)
52. V. Krishnakumar, V. Balachandran, Spectrochim Acta A **63**, 464 (2006)
53. A. Kunduracıoğlu, Ö. Tamer, D. Avcı, İ. Kani, Y. Atalay, B. Çetinkaya, Spectrochim Acta A **121**, 35 (2014)
54. G. Socrates, *Infrared characteristic group of wavenumbers* (Wiley Interscience, New York, 1980)
55. V. Balachandran, V. Karunakaran, Spectrochim Acta A **106**, 284 (2013)
56. Ö. Tamer, D. Avcı, Y. Atalay, Spectrochim Acta A **136**, 644 (2015)
57. D. Lin-Vien, N.B. Colthup, W.G. Fateley, J.G. Grasselli, *The handbook of infraredand raman characteristic frequencies of organic molecules* (Academic Press, Boston, MA, 1991)
58. L.J. Bellamy, *The infrared spectra of complex molecules*, vol. 2 (Chapman and Hall, London, 1980)
59. R. Shanmugam, D. Sathyanarayana, Spectrochim Acta A **40**, 757 (1984)
60. V. Balachandran, K. Parimala, J Mol Struct **1007**, 136 (2012)
61. C.S. Hsu, Spectrosc Lett **7**, 439 (1974)
62. S. Muthu, G. Ramachandran, E. Isac Paulraj, T. Swaminathan, Spectrochim Acta A **128**, 603 (2014)

63. T. Rajamani, S. Muthu, M. Karabacak, Spectrochim Acta A **108**, 186 (2013)
64. R. Zhang, B. Dub, G. Sun, Y. Sun, Spectrochim Acta A **75**, 1115 (2010)
65. M. Szafran, A. Komasa, E.B. Adamska, J Mol Struct (THEOCHEM) **827**, 101 (2007)
66. S. Sebastian, N. Sundaraganesan, Spectrochim Acta A **75**, 941 (2010)
67. Ö. Tamer, D. Avcı, Y. Atalay, J Mol Struct **1098**, 12 (2015)
68. S. Altürk, Ö. Tamer, D. Avcı, Y. Atalay, J Organomet Chem **797**, 110 (2015)